Ultraviolet-visible imagery and spectra of the Fluxus-1 and -2 artificial plasma jets

R. E. Erlandson[1], P. K. Swaminathan[1], C.-I. Meng[1], B. J. Stoyanov[1], J. I. Zetzer[2], B .G. Gavrilov[2], Yu. N. Kiselev[2], and Yu. A. Romanovsky[3]

Abstract. Two active geophysical rocket experiments, known as Fluxus-1 and Fluxus-2, were conducted to study the interaction of artificial aluminum plasma jets with the ionosphere. The plasma jets were generated at night without the aid of solar illumination using specially designed shaped-charge generators. In this paper we present observations from the space-based ultraviolet and visible sensors on the Midcourse Space Experiment (MSX) satellite. Spectrographic imagers on MSX were used to acquire an ultraviolet and visible spectrum of the shaped-charge event and plasma jet evolution. The spectrum contained Al II (Al+) line emissions, Al I line emissions, continuum emissions due to AlO formed through reactions of Al dimers $(Al)_x$ with atomic oxygen, and atmospheric emissions associated with O I and O II. The atmospheric emission features persisted for a few seconds while the Al I and II features were observed during the first frame (0.5s). The plasma jet evolved into a long-lasting luminous plasma cloud that was observed for over 70s from MSX and 3 minutes on the ground. The source of this cloud is most likely emissions from HAlOH.

1. Introduction

Active plasma jet experiments have been used to study a number of problems fundamental to space plasma physics. A major theme has been the study of plasma beam propagation and the closely related topic of beam neutralization. For example, Hausler et al. [1986] proposed a model of plasma beam neutralization involving field-aligned currents that couples to the ionosphere and outer magnetosphere.

The Fluxus-1 and -2 experiments were specifically designed to study the formation and subsequent development stages of an artificial plasma jet. The plasma jet was generated by a shaped-charge device via high explosive at night (without the aid of ionization due to solar illumination) [Adushkin et al., 1993; Kozlov and Smirnova, 1993]. It is believed that the shaped-charge device produces a primary plasma jet that rapidly recombines to form a high-speed neutral jet that undergoes charge exchange reactions and collisions with the ionosphere and atmosphere, resulting in the generation of a secondary plasma jet. The plasma jet comes to rest in the ionosphere, forming a long-lived plasma cloud. The absence of solar illumination facilitates the observation of

[1]The Johns Hopkins University Applied Physics Laboratory, Johns Hopkins Road, Laurel, MD 20723, USA
[2]Institute for Dynamics of Geospheres, Moscow, Russia
[3]Institute of Applied Geophysics, Moscow, Russia

visible radiation from the jet and from jet interactions with the atmosphere and ionosphere. Such observations are discussed in this paper.

2. Experiment Overview

Two scientific payloads were launched eastward from Kapustin Yar, Russia as part of the Fluxus-1 and -2 experiments on January 31, 1997, and February 5, 1997, respectively [see overview by Zetzer et al., 1999, this issue]. The experiments occurred in darkness (no sun and new moon) under quiet geomagnetic conditions at 0500 LT. The rocket contained an instrument payload and the explosive type shaped-charge generator (ETG) payload, which separated from the instrument payload on the upleg of the trajectory. The experiment was observed using optical sensors on the ground, on aircraft, and from space using the Midcourse Space Experiment (MSX) satellite [Mill et al., 1994]. MSX was 3000 km to the south of the experiment.

The ETG was detonated near apogee at an altitude of 140 km, producing a high-speed aluminum plasma jet oriented to within 30° of the magnetic field and back toward the diagnostic payload [Zetzer et al., 1999]. The ETG was designed to produce a plasma jet of total mass 22 g, velocities of 7–40 km/s, and a total kinetic energy of ~3 MJ. Laboratory tests indicate that 92% of the jet energy is confined to within 20° of the jet axis. Gavrilov et al. [1998] showed that the plasma jet produced a diamagnetic depression in the magnetic field, consistent with a peak plasma pressure of 4.7×10^9 (Fluxus-1) and 5.5×10^9 eV/cm^3 (Fluxus-2). This implies a plasma density greater than 1×10^9 cm^{-3}, assuming a plasma jet temperature of 1 eV [Gavrilov et al., 1998].

3. Plasma Jet/Cloud Visible Imagery

The visible signatures (450 – 900 nm) of the Fluxus plasma jets were observed in data collected by the MSX space based visible (SBV) camera at a rate of 1 frame per second. The SBV camera used a 420 x 420 pixel array with an instantaneous field of view of 60 µr x 60 µr resulting in a footprint of 180 x 180 m at a range of 3000 km. Figure 1 contains the initial bright flash associated with the plasma jet and it's interaction with the ambient environment during the Fluxus-2 experiment (Fluxus -1 was similar and is not shown). The shape of the cloud is an ellipse oriented diagonally in the image. The major axis is in the direction of plasma jet propagation, where the location of the brightest pixel is the location of the ETG at the time of the detonation. Visible emissions from the plasma cloud

were recorded for 3 minutes using ground-based cameras [Zetzer et al., 1999] and 75 s using the MSX SBV camera.

The total integrated intensity of the plasma jet during the Fluxus-1 and -2 missions is shown in Figure 2. The background has been subtracted, and frames with stars superimposed on the plasma cloud were not included in Figure 2. The plasma cloud intensity peaks at 1.2 kW/sr during the first image and then drops rapidly. The intensity then begins to rise after reaching a minimum 5 s after ETG detonation, suggesting that two different processes occur. The first emission feature is associated with the ETG detonation and the initial plasma jet expansion. This decays within seconds after the event. In fact, high-speed ground-based photometer data showed that the brightest emissions from the jet were observed for only ~0.1 s [Zetzer et al., 1998]. The second feature, referred to as the plasma cloud, maximized in intensity 20-35 s after the detonation. Figure 2 shows that there is significant intensity in the plasma cloud 80 s after the ETG detonation, indicating an estimated decay time constant of ~100 s. The plasma cloud was circular and grew slowly in size, reaching a diameter of 2 km in a time of 75 s. The plasma cloud source is discussed below.

4. Plasma Jet Spectral Features

The ultraviolet/visible imaging and spectrographic imaging (UVISI) instrument on MSX consists of four imaging and five spectrographic imaging sensors (SPIMs), each commanded to collect images at a rate of 2 Hz [Carbary et al., 1994]. The five SPIMs cover
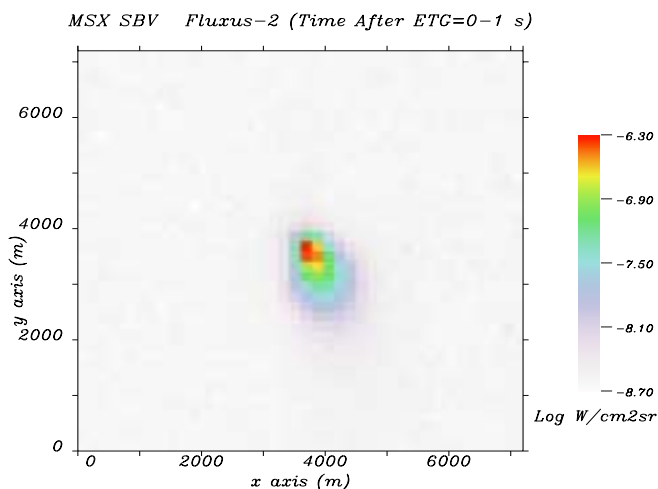

Figure 1. SBV visible image of the plasma jet during Fluxus-2.
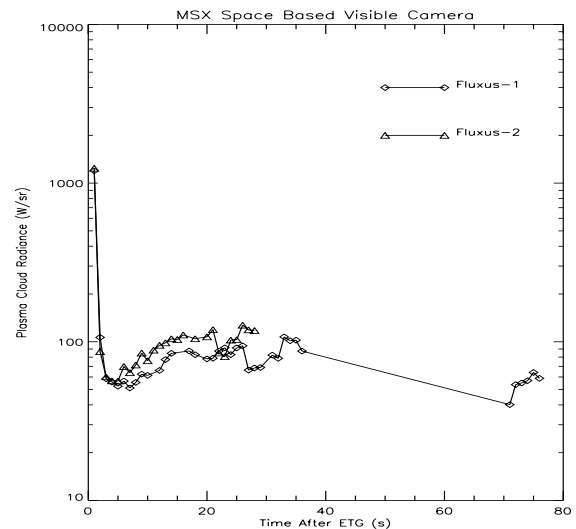

Figure 2. Total plasma cloud intensity (I) from the MSX SBV visible camera during Fluxus-1 and -2. The small decreases in intensity at 25 s (Fluxus-1) and 21 s (Fluxus-2) are due to changes in the MSX slew rate. The data gap from 35 to 70 s occurs during an MSX attitude maneuver.

wavelengths from 113 to 902 nm, each with 272 spectral elements. The SPIMs can be scanned to produce a two-dimensional image, although the sensors were not scanned in this case. The instantaneous field of view of the SPIMs is $0.1 \times 1.5°$ and was centered on the ETG at the time of the detonation, aided by a radio-frequency beacon placed on the rocket and a beacon receiver on the MSX spacecraft [Mill et al., 1994].

The UVISI SPIMs acquired spectra of the artificial plasma jet during both the Fluxus-1 and Fluxus-2 experiments. The experimental setup and conditions were similar during both experiments. Correspondingly, the spectra were qualitatively similar. Thus we show only the spectra from Fluxus-2 (Figure 3). The five panels in Figure 3 cover the spectral range 125–900 nm. The spectra in Figure 3 were determined from a spectrographic image (not shown) with one spectral and one spatial dimension. The plasma jet emissions were localized to a portion of the one spatial dimensional of the spectrographic image was easily distinguished from background emissions that occur over the entire spatial dimension of the image. Most of the plasma jet spectral features were observed during only the first 0.5s frame. The one exception is emissions at 557.7 nm that persisted for ~5 seconds. This is consistent with ground-based observations, which show that plasma jet visible intensity drops by almost 2 orders of magnitude in a time of 0.1 s.

Aluminum neutral and ion features were expected, as the shaped-charge device contained aluminum tubes that were vaporized in the explosion. The experiment was conducted at an altitude of 140 km, mid-latitudes, and a local time of 0500 in a neutral atmosphere containing O, N, N_2, and O_2. We discuss the spectrum

14

recorded using each of the five UVISI SPIMs below. For reference, Figure 3 also contains the background nightglow spectrum (5 s average) collected just prior to the ETG experiment.

SPIM1 (125–173 nm)

An aluminum ion feature (Al II) near 167 nm [Kaufman and Martin, 1991] was observed in the SPIM1 spectrum (Figure 3). No higher ionization levels of Al were observed.

The background emissions in the UVISI SPIM1 spectrum were dominated by Lyman alpha HI (121.8 nm) from atmospheric H and by nightglow emissions from OI (130.4 and 135.6 nm). Enhancements in the nightglow OI (135.6) and OI (130.4) were also observed. They are due to electron impact on ambient atomic oxygen. These enhancements returned to background levels 0.5 s after the event.

SPIM2 (162–252 nm)

An Al^+ feature was also observed at 167 nm in the SPIM2 spectrum, a region of the spectrum where SPIM1 and 2 overlap (Figure 3). Other weak Al II features (176-177 nm, 186 nm, 199-202 nm, and 209 nm). In addition, several prominent Al I peaks were associated with the Rydberg series starting at 213 nm ($3s^2 10d$) up to 237 nm ($3s^2 5d$). Two auroral line features were also observed at 247 (O II $^2P^0$) and 214.3 nm (N II), presumably excited by hot electrons in the plasma jet. As expected, the background features due to NO γ and NO δ bands were observed.

SPIM3 (251–388 nm)

Al I emissions were observed at 257, 266, and 309 nm (Figure 3). In addition, a line emission was observed near 345 nm. This feature may come from an Al I emission ($3p^2$ ^4P) and an auroral feature due to N I at 346.6 nm. The feature near 373 nm is assigned to electron impact production of OII ($^2D^0$), an emission expected when O II ($^2P^0$) at 247 nm is present (see the SPIM2 spectrum).

SPIM4 (377–582 nm)

A strong emission was observed between 390 and 400 nm (Figure 3). This feature is mostly due to a strong Al I emission at 395 nm. In addition, the first negative N_2^+ (391.4 nm) band emission, a common auroral feature produced by electron impact on N_2, was also observed although it is weaker than the Al I emission.

The spectrum was enhanced, like a band feature, over most of the SPIM4 spectrum. This enhancement may at least partially be due to the $\Delta v = -1, 0$ sequence of the AlO (B $\rightarrow$ X) transition. Evidence of AlO is also seen in the SPIM5 spectrum and is discussed below. AlO is expected to readily form as Al dimers (Al_x) collide with atomic oxygen. A number of possible Al II line assignments are also indicated in Figure 3.
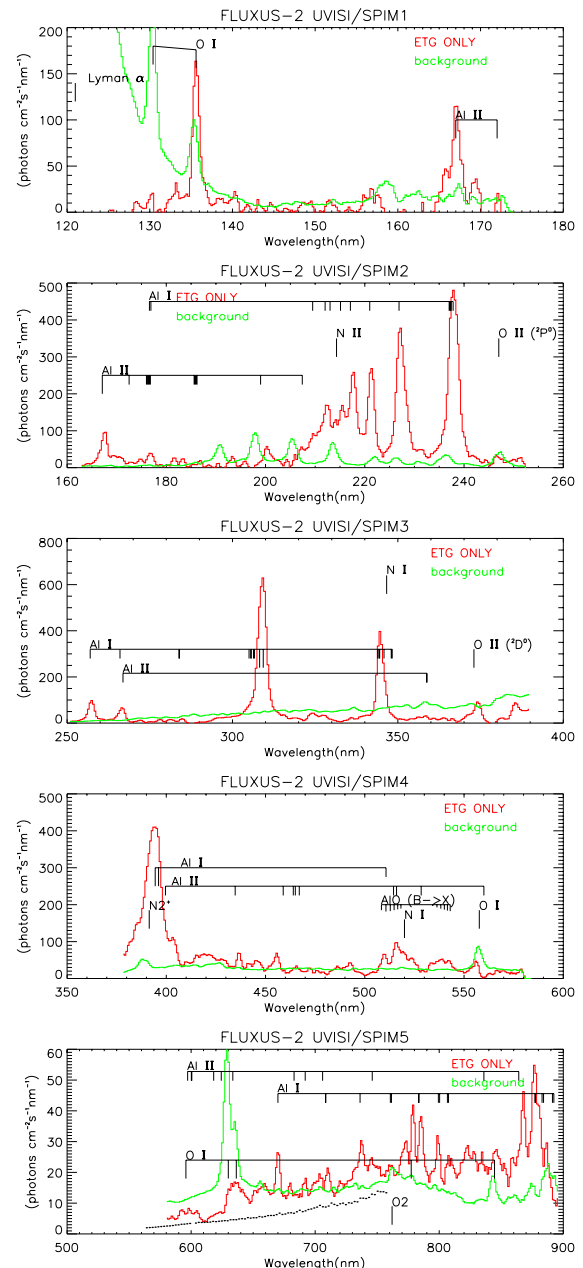

Figure 3. Spectra of the Fluxus-2 artificial plasma jet recorded using the MSX UVISI spectrographic imagers. The dashed line in the SPIM5 spectrum is the predicted continuum emission due to AlO (A $\rightarrow$ X).

A weak line emission was also observed at 557.7 nm due to the OI green-line. Unlike the other emissions, this feature was observed for ~5 s by SPIM4 and peaked in intensity 1.5 s after the ETG detonation (not shown). The Einstein coefficient (lifetime) of the 557.7 nm emission is 1.215 s^{-1} which is consistent with the observed 5 s duration of this emission. The lifetime of this transition, however, is too short to account for the extended plasma cloud emission unless additional energy is pumped into the reaction.

SPIM5 (580–900 nm)

A continuum-like feature was observed in the SPIM5 spectrum (Figure 3). This continuum is due to AlO (A → X) and has been confirmed by matching the underlying continuum in SPIM5 to the spectrum observed by Lindsay and Gole [1977]. In addition, a number of line emissions associated with Al I and Al II are present. Finally, enhancements of the OI (630 nm) line, OI (777.4 nm) line, and OI (844.6 nm) line were observed.

5. Discussion

Spectral observations of Al and Al$^+$ emission confirm that the ETG produced a plasma jet. This is consistent with the in situ observations reported by Zetzer et al. [1999] and Gavrilov et al. [1999] who found that a high-speed, high-density plasma cloud was generated by the ETG at an altitude of 140 km in the absence of solar radiation. Nonetheless, the plasma jet spectrum is dominated by neutral aluminum line emissions, indicating a significant fraction of excited neutral Al in the jet.

A large number of nightglow and auroral emissions were excited during the Fluxus experiments. These emissions are consistent with electron impact excitation of the atmospheric species O, N, N_2, and O_2. The emission at 557.7 nm was observed for up to 5s and peaked 1.5s after the plasma jet injection.

The spectral signature of the long-lasting plasma cloud observed using the broadband SBV camera was too weak to be measured using the UVISI spectrograph. The most likely source of the plasma cloud are emissions from HALOH that are produced as AlO, formed as Al dimers $(Al)_x$ react with atomic oxygen, and H_2O react.

References

Adushkin, V. V., et al., Active geophysical rocket experiments in the ionosphere with the high velocity plasma jet injection, *Doklady RAS. 331*(4), 486–489, 1993.

Carbary, J. F., et al., Ultraviolet and visible imaging and spectrographic imaging instrument, *Appl. Opt., 33*(19), 4201–4213, 1994.

Erlandson, R. E., et al., Initial results from the operation of two argon ion generators in the auroral ionosphere, *J. Geophys. Res., 92*, 4601, 1987.

Gavrilov, B. G., et al., Diamagnetic effect produced by the Fluxus-1 and -2 artificial plasma jet, *Geophys. Res. Lett.*, in press, 1999.

Haerendel, G., and R. Z. Sagdeev, Artificial plasma jet in the ionosphere, *Adv. Space Res., 1*, 29, 1981.

Hausler, B., et al., Observations of the artificially injected Porcupine xenon ion beam in the ionosphere, *J. Geophys. Res., 91*, 287, 1986.

Kaufman, V., and W. C. Martin, Wavelengths and Energy Level Classifications for the Spectra of Aluminum (Al I through Al XIII), *J. Phys. Chem. Ref. Data*, *20*, 775, 1991.

Kozlov, S. I., and N. V. Smirnova, Techniques and means of creating artificial formations in the upper atmosphere: Analysis of characteristics of artificial disturbances, *Cosmic Res., 30*(4), 402–425, 1993.

Lindsay, D. H., and J. L. Gole, Al + O_8 chemiluminescence: Perturbations and vibrational population anomalies in the B$^2\Sigma^+$ state of AlO, *J. Chem. Phys., 66*, 3886, 1997.

Mill, J. D., et al., Midcourse Space Experiment: Introduction to the spacecraft, instruments and scientific objectives, *J. Spacecr. Rockets, 31*(5), 900–907, 1994.

Moore, T. E., et al., Anomalous auroral electron distributions due to an artificial ion beam in the ionosphere, *J. Geophys. Res., 87*, 7569, 1982.

Zetzer, J. I., et al., The Fluxus-1 and -2 experiment: Investigation of plasma jet dynamics and interactions with the ionosphere, *Spacecraft Charging Technology Conference Proceedings*, 1999.

R. E. Erlandson et al., The Johns Hopkins University Applied Physics Laboratory, Laurel, MD, USA. (email: erlandson@jhuapl.edu)

J. I. Zetzer, et al., Institute for Dynamics of Geospheres, Russian Academy of Sciences, Leninsky prosp. 38, korp. 6, Moscow, Russia, 117939. (email: zetzer@idg.chph.ras